Nuclear structure effects in k^+ elastic scattering from ^{3}He, ^{3}H, ^{4}He, and ^{12}C

Manuel J. Páez* and Rubin H. Landau
Department of Physics, Oregon State University, Corvallis, Oregon 97331
(Received 20 April 1981)

The elastic scattering of positive kaons from ^{12}C, ^{3}He, ^{3}H, and ^{4}He is calculated with a theoretical momentum space optical potential. The theory includes nuclear spin, nucleon recoil and binding, a Lorentz invariant angle transformation, realistic nuclear form factors for the proton and neutron matter and spin distributions, and a kaon-nucleon T matrix with off-shell behavior based on a separable potential model. Differential and total cross sections, polarizations, and isotopic ratios are examined for kaon energies from 0.4 to 1 GeV and compared with results from pion and electron scattering.

[NUCLEAR REACTIONS ^{12}C(K^+,K^+), ^{4}He(K^+,K^+), ^{3}He(K^+,K^+), ^{3}H(K^+,K^+), ^{3}He(K^0,K^0); $E = 39-804$ MeV; $\sigma(\theta)$ and σ_{tot}; theoretical calculation, momentum space optical potential; spin effects, binding, recoil, angle transformation; compare with ^{12}C data.]

I. INTRODUCTION

Interest in kaon-nucleus scattering arises from a desire to learn more about the kaon-nucleon (KN) interaction, more about nuclear structure, more about the kaon-nucleus interaction, or a combination of these. Since the K^+ and K^- have different strangeness, scattering of $K^\pm$ beams from a proton target cannot determine the complete KN amplitude, and a nuclear (deuterium) target must be used to deduce kaon-neutron cross sections.[1] Although this technique has its uncertainties,[2] there are no viable alternatives and therefore studies of the K-N and K-nucleus problem are closely related.

The use of kaons as a nuclear probe, in particular, using K^+'s to deduce neutron distributions in nuclei, has been advocated a good number of times[3-10] on the basis of their high nuclear penetrability ($\lambda \approx 6$ fm), their relatively simple and elementary interaction with the nucleus (the single scattering impulse approximation), and the unique energy and angular momentum dependence of the K^+N amplitude. Although at present the elementary KN amplitude (particularly the neutron part) is not known with enough precision to permit a reliable extraction of neutron distributions,[3,5-7] our knowledge should improve in the future with the construction of dedicated beam lines or kaon factories. Whether one should *then* truly believe the accuracy of the neutron sizes deduced with strongly interacting probes is a somewhat different question (we assume charge distributions, and thus proton sizes are determined best from electron scattering). We advocate the use of as many strongly interacting probes as possible to study a nucleus. If it is then possible to obtain a consistent and statistically significant agreement with all these data—especially using the same nuclear structure and theoretical framework—then the deduced size will be "believable." Of course the existence of meson currents within nuclei, and our less-than-fundamental description of two body forces without quark degrees of freedom,[11] may restrict the limits of precision of any such size determination, but that situation should improve in the very near future.

In this paper, we begin to develop this unified theory of nuclear reactions by extending our previous developments in the momentum-space description of pion[12-14] and nucleon[15] elastic and charge exchange scattering from nuclei to also include kaon scattering.[16] In the work presented here we concentrate on K^+ elastic scattering from the mirror nuclei ^{3}He and ^{3}H for kinetic energies in the range $40-1000$ MeV (^{12}C and ^{4}He are also studied). In subsequent publications we present our results on the ^{3}H(K^+,K^0) ^{3}H reaction,[17] K^- scattering, and a truly unified study of $\pi^\pm$, N, and $K^\pm$ scattering from selected nuclei.

The study reported upon here is new in its being the first kaon study of the helium isotopes, in its inclusion of *KN*, *S*, *P*, and *D*, and *F* waves—with their full angular dependence, in its careful inclusion of the spin dependent amplitudes and densities, in its examination of the full energy range from zero to 1 GeV, and in its consistent two body and many body dynamics (Lippmann-Schwinger equation with relativistic kinematics). In addition, the off-energy shell behavior of the K^+N amplitudes is determined by a separable potential model.

A limitation of the present calculation is our use of mainly the Martin[18] K^+N amplitudes. We do know, however, that low energy K^+ nucleus scattering is very sensitive to uncertainties in the K^+N scattering lengths—as shown by Hetherington or Schick[19] some sixteen years ago—and that this input sensitivity continues into the medium energies, as shown by Cotanch,[6–8] Tabakin,[6,9,10] Rosentahl,[9,10] Dover,[3–5] Walker,[4,5] and Moffa.[3] We do not repeat our (rather expensive) calculations using the BGRT *KN* analysis[20] since previous work provides adequate documentation of the significant changes which occur, and since it appears the BGRT amplitudes no longer fit all available *KN* data.[21] We have, however, run with the very new *KN* phases of Watts *et al.*[20]

II. THEORY

A. Optical potential

We calculate kaon-nucleus (*KA*) scattering amplitudes by solving the Lippman-Schwinger integral equation for spin $0 \times \frac{1}{2}$ scattering

$$T'_{L\pm}(k'\,|\,k) = U_{L\pm}(k'\,|\,k) + \frac{2}{\pi}\int_0^\infty \frac{dp\,p^2 U_{L\pm}(k'\,|\,p)T'_{L\pm}(p\,|\,k)}{E-(m_K{}^2+p^2)^{1/2}-(m_A{}^2+p^2)^{1/2}+i\epsilon} \ . \tag{1}$$

Here $\vec{k}$ and $\vec{k}'$ are the initial and final kaon momenta, $E = E_K(k_0) + E_A(k_0)$ is the *K*-*A* c.m. energy, the complex optical potential U is nonlocal, energy dependent, and spin dependent, and the angular momentum is $J = L \pm \frac{1}{2}$, Since U is constructed from elementary K^+N amplitudes, and a solution of Eq. (1) is equivalent to summing the Born series, $T_{L\pm}$ will contain all orders of multiple spin-flip and nonflip scattering. A general description of the optical potential we use in Eq. (1) has been given before[12,13] for pion scattering and will not be repeated here. The potential $U_{L\pm}$ is a linear combination of central and spin-dependent terms

$$U_{L\pm}(k'\,|\,k) = \frac{2\pi^2}{2L+1}\left[U_C^L + \begin{Bmatrix} L \\ -(L+1)\end{Bmatrix} U_S^L\right] \ . \tag{2}$$

In the impulse and factorization approximation, the matrix elements of U are

$$U_C(\vec{k}'\,|\,\vec{k}) = \frac{A-1}{A}[\langle f\,|\,t^{Kp}(\omega)\,|\,i\rangle Z\rho^p_{\text{matter}}(q) + \langle f\,|\,t^{Kn}(\omega)\,|\,i\rangle N\rho^n_{\text{matter}}(q)] \ , \tag{3}$$

$$U_S(\vec{k}'\,|\,\vec{k}) = \frac{A-1}{A}[\langle f\,|\,t^{Kp}_{\text{flip}}\,|\,i\rangle Z\rho^p_{\text{spin}}(q) + \langle f\,|\,t^{Kn}_{\text{flip}}(\omega)\,|\,i\rangle N\rho^n_{\text{spin}}(q)]i\vec{\sigma}\cdot(\hat{k}\times\hat{k}') \ , \tag{4}$$

where

$$|\,i\rangle = |\,\vec{k},\vec{p}_0\rangle,\ \ |\,f\rangle = |\,\vec{k}',\vec{p}_0{}'\rangle,\ \ \vec{p}_0{}' = \vec{p}-\vec{q},\ \ \vec{q} = \vec{k}'-\vec{k} \ , \tag{5}$$

the ρ's are appropriate nuclear form factors, and $\vec{p}_0$ is the "optimal" choice of momentum for the struck nucleon,

$$\vec{p}_0 = -\frac{\vec{k}}{A} + \frac{A-1}{2A}\vec{q} \ . \tag{6}$$

The T matrices in Eqs. (1)–(5) are in the *K*-*A* c.m., we relate them to those in the *KN* c.m. $\langle \vec{\kappa}'\,|\,t(\tilde{\omega})\,|\,\vec{\kappa}\rangle$, via the transformations

$$\langle \vec{k}',\vec{p}_0{}'\,|\,t(\omega)\,|\,\vec{k},\vec{p}_0\rangle = \gamma\langle \vec{\kappa}\,|\,t(\tilde{\omega})\,|\,\vec{k}\rangle \ , \tag{7}$$

$$\gamma = \left[\frac{E_K(\kappa)E_K(\kappa')E_N(\kappa)E_N(\kappa')}{E_K(k)E_K(k')E_N(p_0)E_N(p_0')}\right]^{1/2} \ . \tag{8}$$

The two-body c.m. momentum $\vec{\kappa}$ and $\vec{\kappa}'$ are calculated by separately evaluating the incoming and outgoing c.m. energy $\sqrt{s}$ for the initial $|\vec{k},\vec{p}_0\rangle$ and final $|\vec{k}',\vec{p}_0'\rangle$ states, e.g., $s_{in}=(k+p_0)^2$, $s_{out}=(k'+p_0')^2$,

$$\begin{aligned}
\vec{\kappa} &= \vec{Q} - \{\vec{Q}\cdot\vec{K}/K_0[K_0+(s_{in})^{1/2}]\}\vec{K} \ , \\
2\vec{Q} &= \vec{k} - \vec{p}_0 - [(m_K{}^2 - m_n{}^2)/s_{in}]\vec{K} \ , \\
K &= (K_0,\vec{K}) = [E_K(k)+E_N(p_0),\ \vec{k}+\vec{p}_0] \ ,
\end{aligned} \tag{9}$$

with a similar relation for $\vec{\kappa}'$. Since s (energy) need not be conserved in these collisions, this amounts to a different Lorentz transformation for the incoming and outgoing states. However, this procedure is completely covariant and unique and if we define the scattering angle in the KN c.m. (the "angle transformation") via[22,23]

$$\vec{\kappa}'\cdot\vec{\kappa} = \kappa'\kappa\cos\theta_{KN} = \left\{\vec{Q} = \frac{[\vec{Q}\cdot\vec{K}]\vec{K}}{K_0[K_0+(s_{in})^{1/2}]}\right\}\cdot\left\{\vec{Q}' - \frac{[\vec{Q}'\cdot\vec{K}']\vec{K}'}{K_0'[K_0'+(s_{out})^{1/2}]}\right\} , \tag{10}$$

then $|\cos\theta_{KN}|$ will always be ≤ 1 for arbitrary values of k' and k. (The "no angle transformation" recipe would amount to choosing $\cos\theta_{KN}\approx\cos\theta_{KA}$.)

The K-nucleon subenergy $\tilde{\omega}$ in Eq. (7) is chosen according to one of two prescriptions—the different possible prescriptions reflecting the ambiguity present in a theory which employs off-energy shell amplitudes. The first prescription, $\tilde{\omega}=\tilde{\omega}_{3B}$, is based on a three body formulation of the first order optical potential[22] in which there is a projectile of momentum $\vec{k}$, an active nucleon with $\vec{p}+\vec{p}_0$, and a passive core with momentum $\vec{P}=-\vec{k}-\vec{p}-\vec{p}_0$. One then calculates the KN c.m. energy by taking the energy of the kaon plus *nucleus* and subtracting from it the energies of (1) the A-1 core, (2) the motion of the KN c.m., and (3) the "effective" binding energy of the active nucleon. In the nonrelativistic nucleon limit, $\tilde{\omega}_{3B}$ has the familiar form

$$\omega_{3B}\simeq E_K(k)+m_N+k^2/2Am_N - P^2/2(A-1)m_N - P^2/2(E_k(k)+m_N) - |E_B| \ . \tag{11}$$

In the present survey calculation, we have kept $|E_B|$ fixed at 5 MeV and set $p^2/2\mu$ equal to some average value, 16 MeV.[22] Although this amounts to a total downward shift in subenergy of ~ 20 MeV, the slow variation of the KN amplitudes with energy make the details unimportant.

Our second choice of energy (which would agree with the first if we had on-shell scattering) is a more conventional two body center-of-mass energy,

$$\omega=\sqrt{s}=\omega_0=[(P_K^\mu+P_N^\mu)^2]^{1/2}=[m_K{}^2+m_N{}^2+2E_K(k)E_n(p_0)-2\vec{k}\cdot\vec{p}_0]^{1/2} \ . \tag{12}$$

These "optimal" choices require the KN T matrix to be evaluated at an energy which increases with the K-nucleus scattering angle ($\vec{p}_0$ depends on momentum transfer). In addition, Eqs. (1), (3), (9), and (11) require an independent variation of both momentum variables $\vec{k}$ and $\vec{k}'$ ($0\leq k,k'\leq\infty$), and a separate variation of the energy ω. These requirements are included in a straightforward manner since we calculate the optical potential in momentum space, and use a separable model for the off-shell behavior in each eigen channel α of the KN T matrix

$$\langle\kappa'|t^\alpha[\omega(\kappa_0)]|\kappa\rangle = \langle\kappa_0|t^\alpha[\omega(\kappa_0)]|\kappa_0\rangle\frac{g_\alpha(\kappa')g_\alpha(\kappa)}{g_\alpha(\kappa_0)^2} \ . \tag{13}$$

Dover and Walker[4] have found that K^+-nucleus scattering displays very little sensitivity to the actual form of the separable potential $g(p)$. We have confirmed their finding by varying the g's in Eq. (13) and letting $g_\alpha\to 1$. (Since there is a low sensitivity to the form of g, we actually used a modified form of πN potentials appropriate for each eigenchannel.)

B. K^+N amplitudes

The on-shell amplitudes are calculated with the Martin phase shifts,[18] since his appears to be the best complete analysis currently available. There are, however, large uncertainties in the $I=0$ (neutron) amplitudes, and we have also made some calculations with the recent analysis by Watt *et al.*[20] In Figs. 1 and 2 we show the S-F wave K^+p and K^+n scattering amplitudes as they are used in our calculation (i.e., including the angu-

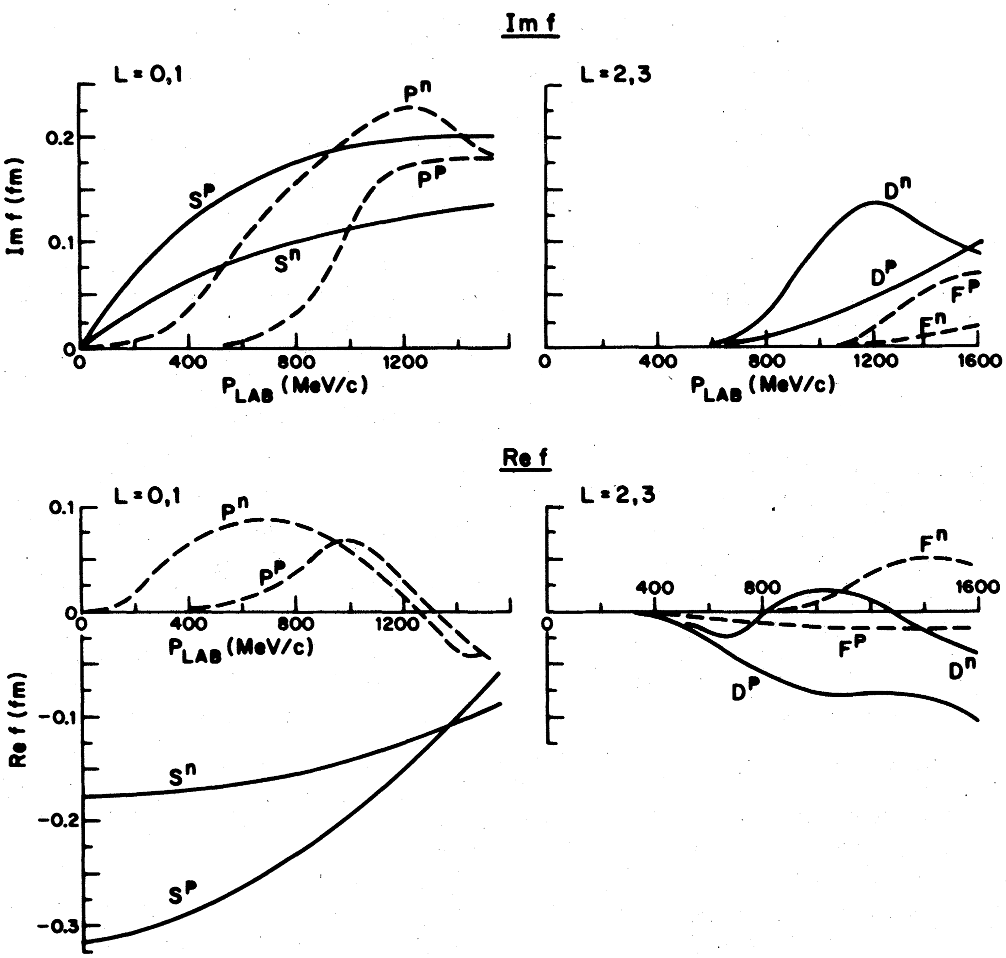

FIG. 1. Real and imaginary parts of the K^+ neutron (n) and proton (p) scattering amplitudes for the $L = 0, 1, 2, 3$ (S,P,D,F) partial waves.

lar momentum weighting):

$$f_l = (l+1)h_{l+}(\kappa_0) + l h_{l-}(\kappa_0) \ , \tag{14a}$$

$$f_l^{\text{flip}} = h_{l+}(\kappa_0) - h_{l-}(\kappa_0) \ . \tag{14b}$$

$$h_{J=l\pm 1/2}(\kappa_0) = \eta_\alpha(\kappa_0)\{\exp[2i\delta_\alpha(\kappa_0)] - 1\}/2i\kappa_0, \quad \alpha = \{L,J,I\} \ . \tag{15}$$

We see that the $l = 0$ nonflip proton amplitude dominates for $P_{\text{lab}} \lesssim 800$ MeV/c (Fig. 1), whereas for $P_{\text{lab}} \gtrsim 900$ MeV/c the P wave neutron nonflip amplitude dominates. Furthermore, we see in Fig. 1 that the real parts of the nonflip amplitudes are always dominated by the repulsive S waves for $T^K \lesssim 800$ MeV, and that the P waves are attractive but very weak.

In Fig. 2 we see that the spin-flip amplitudes for P waves are quite different in behavior from the nonflip amplitudes (there is no S wave spin-flip), with the P wave *proton* amplitudes now dominating and the real parts being quite large. Specifically, the destructive cancellation which occurs in f_l, Eq. (14a), when the P_{11} and P_{13} amplitudes are added,[18] becomes constructive when they are subtracted to form the spin flip amplitude, Eq. (14b). (To a lesser extent this is also true for the P_{01} and P_{03} eigenchannels). Finally, we can see in Figs. 1 and 2 that while the D and F waves may be significant, they never dominate.

Since (K^+,K^0) and (p,n) are both isodoublets, the strong interaction T matrices are related by

$$T^{\text{el}}(K^+p) = T(I=1) = T^{\text{el}}(K^0n) \ , \tag{16a}$$

$$T^{\mathrm{el}}(K^+n) = \tfrac{1}{2}[T(1) + T(0)] = T^{\mathrm{el}}(K^0p) \ , \tag{16b}$$

$$T(K^+n \rightarrow K^0p) = T^{\mathrm{el}}(K^+p) - T^{\mathrm{el}}(K^+n) \ , \tag{16c}$$

so all of these amplitudes are known. The charge exchange amplitudes, shown by Dover and Moffa,[3] are somewhat smaller than the neutron ones.

C. Form factors

To calculate the first order optical potential Eqs. (3)–(5) for a spin zero nucleus, only the matter form factors are required and for ^{12}C and ^{4}He we can even set the n and p distributions equal to the charge form factor with proton size removed. We remove the proton size from the ^{4}He charge form factor of Frosch *et al.*[24] by explicit division by the proton form factor $f_c(q)$ (Ref. 25)

$$\rho^p_{\mathrm{matter}}(^4\mathrm{He}) = [1 - (a^2q^2)^6]e^{-b^2q^2}/f_c(q), \tag{17}$$

$$f_c(q) = (1 + q^2/x)^{-2}, \ \ (a,b) = (0.316, 0.681) \ \mathrm{fm}, \ \ x = 18.2 \ \mathrm{fm}^{-2} \ . \tag{18}$$

For ^{12}C we use the fit of Sick and McCarthy[26] and remove the proton size [$r_{\mathrm{rms}} = 0.81$ fm (Ref. 25)] from the a_{CH} parameter:

$$\begin{gathered} \rho^p_{\mathrm{matter}}(^{12}\mathrm{C}) = [1 - \alpha(qa_{\mathrm{CM}})^2/2(2+3\alpha)]e^{-q^2a_{\mathrm{CH}}{}^2/4} \\ (a_{\mathrm{CH}}, a_{\mathrm{CM}}) = (1.51, 1.60) \ \mathrm{fm}, \ \ \alpha = (A-4)/6 \ . \end{gathered} \tag{19}$$

To evaluate the optical potential for the spin $\frac{1}{2}$ three nucleon system it is necessary to know the p and n matter and spin form factors for ^{3}He and ^{3}H. Since ^{3}He and ^{3}H form an isodoublet with a totally antisymmetric wave function in the space-spin-isospin coordinates of the three nucleons, it is possible to treat both nuclei simultaneously. We give the results for ^{3}He, with the understanding that the ^{3}H form factors are obtained by the interchange $p \rightleftarrows n$.

By examining the original work of Gibson and Schiff,[27] we have indicated[13] previously that these form factors can be related to the large, fully symmetric component of the $3N$ wave function, S, the small ($\sim 2\%$) mixed symmetry component, S', and the small ($\sim 5\%$) mixed D state. These relations are indicated in the first (a) lines of Eqs. (20)–(23). Since only three of the electromagnetic form factors for the $3N$ systems are known (there are essentially no data on the magnetic form factor of ^{3}H) some assumptions are necessary to determine the four hadronic form factors. If we follow Gibson's analysis[27] it seems safe to ignore the small DD terms and use a single, effective SD component. In this case [and with the assumptions of zero charge form factor for the neutron, $\mu(^3\mathrm{He}) = \mu_n$, and no exchange currents], we obtain the second (b) lines of Eqs. (20)–(23):

$$\rho^p_{\mathrm{matter}}(q) = F_{1C}(SS,DD) - F_{2C}(SS',DD)/2 \tag{20a}$$

$$\simeq F_{\mathrm{charge}}(^3\mathrm{He})/f_c(p) \ , \tag{20b}$$

$$\rho^n_{\mathrm{matter}}(q) = F_{1C}(SS,DD) + F_{2C}(SS',DD) \tag{21a}$$

$$\simeq F_{\mathrm{charge}}(^3\mathrm{H})/f_c(p) \ , \tag{21b}$$

$$\rho^n_{\mathrm{spin}}(q) = F_{1M}(SS',SD,DD) + F_{2M}(SS',SD,DD) \tag{22a}$$

$$\simeq \frac{\mu_N}{2(\mu_p + 2\mu_n)f_c(p)} \left\{ 2F_{\mathrm{mag}}(^3\mathrm{He}) + \frac{\mu_p}{3\mu_n}[4F_c(^3\mathrm{He}) - F_c(^3\mathrm{H})] \right\} \ , \tag{22b}$$

$$\rho^p_{\mathrm{spin}}(q) = F_{2M}(SS',SD,DD)/2 \underset{q\rightarrow 0}{(\rightarrow 0)} \tag{23a}$$

$$\simeq \frac{\mu_n}{2(\mu_p + 2\mu_n)f_c(p)} \{F_{\mathrm{mag}}(^3\mathrm{He}) - \tfrac{1}{3}[4F_c(^3\mathrm{He}) - F_c(^3\mathrm{H})]\} \ , \tag{23b}$$

$$\mu_p = 2.793\mu_N, \ \ \mu_n = -1.913\mu_N \ . \tag{23c}$$

We see that the $p(n)$ matter form factor contains both large and small components and is directly proportional to the charge form factor of ^{3}He(^{3}H). In turn, the p spin form factor contains only small components, whereas the n spin form factor has both large and small parts. Since both these spin form factors are related to differences of the charge and magnetic moment form factors [sign $(\mu_p) = -$sign (μ_n)], they are very sensitive to the uncertainties in the electromagnetic form factors, and our hope is that meson scattering may provide useful information on the nuclear structure. A caveat necessary to mention at this point is that we know mesonic exchange currents contribute significantly to the electromagnetic form factors and that there is no reason for them not to contribute in even different ways to the hadronic form factors.

For ^{3}He we use the analytic forms for the charge and magnetic form factors which McCarthy *et al.*[28] fit to their electron scattering data:

$$F_{c,m}(^3\text{He}) = \exp[-a^2q^2] - b^2q^2\exp(-c^2q^2) + d\exp\left[-\left[\frac{q-q_0}{p}\right]^2\right] \tag{24a}$$

$$a_c = 0.675 \pm 0.008 \text{ fm}, \; b_c = 0.366 \pm 0.025 \text{ fm}, \; c_c = 0.836 \pm 0.032 \text{ fm}, \; d_c = (-6.78 \pm 0.83) \times 10^{-3} \; ,$$

$$q_0 = 3.98 \pm 0.09 \text{ fm}^{-1}, \; p_c = 0.90 \pm 0.16 \text{ fm}^{-1} \; , \tag{24b}$$

$$a_m = 0.654 \pm 0.024 \text{ fm}, \; b_m = 0.456 \pm 0.029 \text{ fm}, \; c_m = 0.821 \pm 0.053 \text{ fm}, \; d_m = 0 \; . \tag{24c}$$

For the ^{3}H charge form factor we use the actual data points of Collard *et al.*[29] for $q^2 \le 8$ fm^{-2} and for $8 < q^2 < 16$ fm^{-2} we use a fit to $F_c(^3\text{H})$ with McMillan's three nucleon wave functions[30] (for $q^2 > 16$ fm^{-2} we assume a continuous Gaussian drop off). Since McMillan's wave functions fit $F_c(^3\text{He})$ (for which there are large q^2 data) fairly well in the range $8 < q^2 < 12$ fm^{-2}, our input should be fairly accurate there. Yet if $F_c(^3\text{H})$ [i.e., $\rho^n_{\text{matter}}(^3\text{He})$, $\rho^n_{\text{spin}}(^3\text{He})$] is required for larger q^2, our predictions must be considered unreliable. This would not, however, be an undesirable state of affairs since then K^+ scattering could be used to study unexplored nuclear structure.

Since the ^{3}H form factors are obtained simply via the $p \rightleftharpoons n$ interchange in Eqs. (20)—(23), and since the pure strong K-$3N$ amplitudes have the same isospin structure as the K-N amplitudes, Eq. (16), i.e.,

$$T^{\text{el}}(K^+\,{}^3\text{He}) = T^{\text{el}}(K^0\,{}^3\text{H}), \; T^{\text{el}}(K^+\,{}^3\text{H}) = T^{\text{el}}(K^0\,{}^3\text{He}) \; , \tag{25a}$$

$$T(K^+\,{}^3\text{H} \rightleftharpoons K^0\,{}^3\text{He}) = T^{\text{el}}(K^+\,{}^3\text{He}) - T^{\text{el}}(K^+\,{}^3\text{H}) \; , \tag{25b}$$

all terms in the potential are known. Therefore, it should be possible to isolate the contribution from different parts of the optical potential, Eqs. (3)—(5), by making a judicious choice of target and reaction and thus probe the structure of the $3N$ wave function. In the next section we study the possibility.

III. RESULTS

A. ^{12}C

To check our calculational procedure we first studied K^+-^{12}C elastic scattering for $T^K_{\text{lab}} = 446$ MeV (800 MeV/c). Since this reaction has already been studied theoretically[5,10] by groups at Brookhaven,[3,4] Indiana,[4] Pittsburgh,[6,9] and North Carolina State[7,8] and studied experimentally by a Carnegie-Mellon—Houston—Brookhaven collaboration,[10,31] comparison of our results with those of others was possible. Our results, some of which are shown in Fig. 3, appear quantitatively similar to those of Dover and Walker presented in Ref. 10. In particular, both calculations lie below the forward angle data and both show very little sensitivity to the details of the separable potentials used in Eq. (13) to generate the off-energy-shell behavior of the KN T matrix.

Since our agreement with these data is less than satisfactory, and since other (rather different) optical models appear[10] to obtain more satisfactory agree-

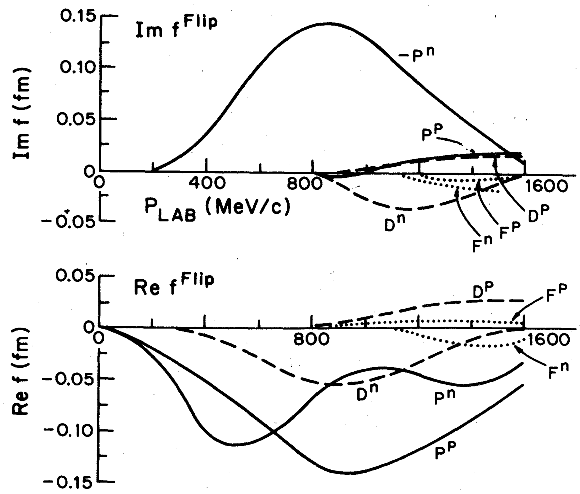

FIG. 2. Same as Fig. 1 except now for the spin flip amplitudes.

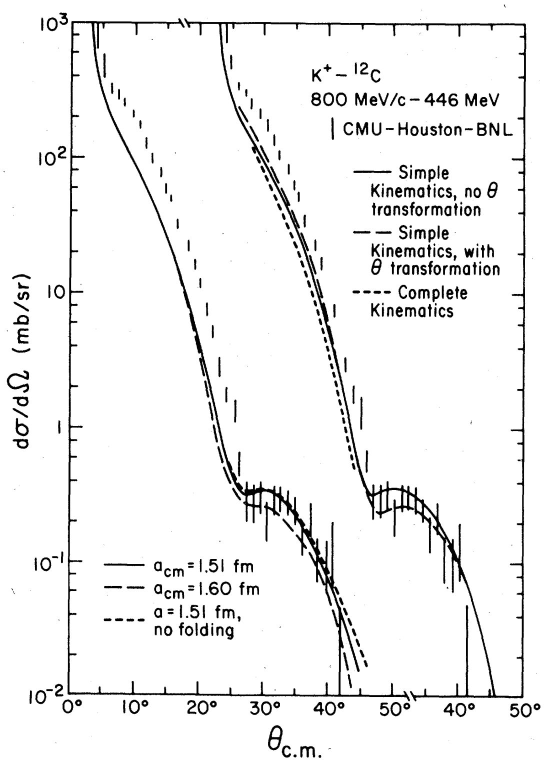

FIG. 3. K^+-^{12}C elastic scattering at 446 MeV compared to the data of the CMU-Houston-BNL group (Refs. 10,31). On the left the results are shown for two different values of the size parameter "a" in the ^{12}C form factor, Eq. (19), and without integration over internal nucleon motion ("no folding"). The curves on the right show the effects of using "simple" kinematics and of including the "angle transformation."

ment, we have examined a number of effects which may change our answers. First, as we see on left of Fig. 3, using a more a recent determination of the form factor of ^{13}C ($a_{\rm CM} = 1.51$ fm in Eq. (19) vs the 1.60 fm used in Ref. 12) is significant, but does not change the answer much for $\theta \lesssim 20°$ where the constructive Coulomb nuclear intereference dominates. Secondly, using a "folding" procedure[12] to Fermi average the elementary KN amplitudes (solid vs heavy dashed curve in the left of Fig. 3) produces only minor changes for the angles considered.

Although not shown, we have also found that (1) the inclusion of KN $D+F$ waves, or (2) the use of an approximate Klein-Gordon equation (we normally use a Lippmann-Schwinger equation with relativistic kinematics), or (3) use of the new Watts *et al.*[18] KN phases produces very minor changes here. However, we have found that the weakness of the nuclear K^+-^{12}C interaction [$\lambda_K \sim 6$ fm (Ref. 8)] means that the Coulomb interaction must be treated carefully. For ^{12}C we have included the Coulomb interaction exactly with a Coulomb potential appropriate to the realistic charge density, Eq. (19).

Since one of the main differences between the momentum space calculations and the coordinate space ones lies in the treatment of kinematics and the amplitude transformations Eqs. (6)–(12), we have displayed the importance of these effects in the right hand part of Fig. 3. We see that the forward cross can be raised by $\sim 40\%$ if we employ "simple kinematics," [instead of Eq. (11) we used Eq. (12) with $\vec{p}_0 = -\vec{k}_0/A$]. If we do not include the "angle transformation" Eq. (10), i.e., set $\cos\theta_{KN} \simeq \cos\theta_{KA}$, the forward peak ($\theta \lesssim 30°$) is lowered by $\sim 20\%$, but the larger angle cross section is raised by $\sim 30\%$ (the opposite effect as occurs for pions).

Since higher order corrections to the theory are likely to be the same or smaller in size than these just considered, the origin of this factor of 2 discrepancy with the K^+-^{12}C data is a bit of a mystery to us. However, since the uncertainties in the K^+N phases can cause changes of this size (although in the wrong direction[6,7] if we use the BGRT[20] analysis), our suspicion is that these low energy phases may change.

B. K^+-^{3}He, K^+-^{3}H (K^0-^{3}He)—General features

Our results for K^+ scattering from unpolarized ^{3}He, ^{3}H, and ^{4}He are presented in Figs. 4 through 14. In general, since the interaction is weak there is little multiple scattering and as we see in Fig. 4 the results from the full solution of the Lippmann Schwinger equation is *quantitatively* similar to the single scattering result [see Eq. (1)]

$$T^{KA} \simeq U(\vec{k}\,'\,|\,\vec{k}) = \sum_{\alpha} t_\alpha^{KN} \rho_\alpha(\vec{k}\,' - \vec{k}) \quad . \quad (26)$$

As is clear in Fig. 5(b), the zero in any one form factor, $\rho_\alpha(q)$, is filled in by the other form factors. Note, however, that Fig. 4 is a highly compressed semilog plot and that the quantitative differences are quite large, especially at low energy. For example, at 39 MeV multiple scattering reduces single scattering by $\sim 50\%$, a truly significant amount in light of the moderate angular dependence. A similar reduction of the single scattering at this energy was found by Hetherington and Schick[19] in their pioneering Faddeev study of K^+d scattering. However, they also found similar changes in the magnitude of the cross section arising from uncertainties in the KN isosinglet scattering length—a difficult quantity to measure even today.

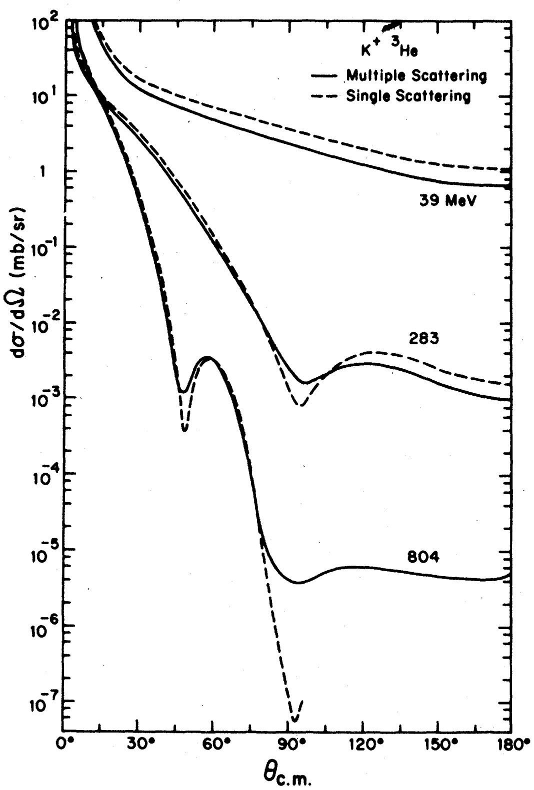

FIG. 4. K^+-^{3}He elastic scattering as calculated by solving the Lippmann-Schwinger equation (multiple scattering) or in first Born approximation (single scattering).

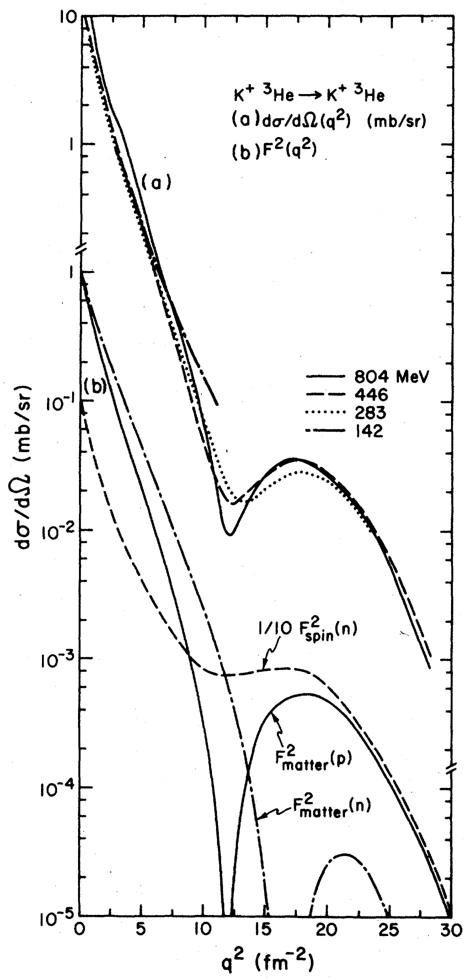

FIG. 5. (a) K^+-^{3}He scattering for $T = 142-804$ MeV plotted as a function of the squared momentum transfer q^2. (b) The squared neutron and proton matter form factors and neutron spin form factor of ^{3}He plotted versus the squared momentum transfer.

To understand better the results of our calculation, in Fig. 5(a) we have replotted some of the K^+ ^{3}He cross sections as a function of momentum transfer squared and in Fig. 5(b) we have plotted on

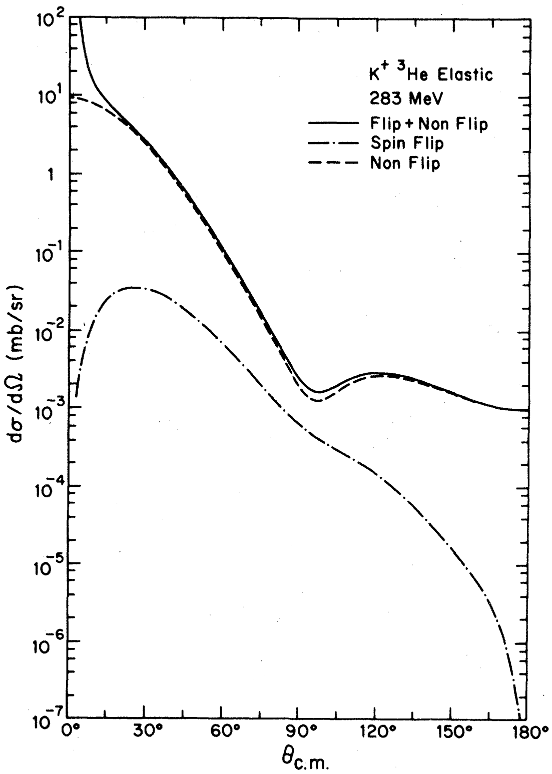

FIG. 6. The contribution of spin flip and nonflip scattering to elastic K^+-^{3}He scattering at 283 MeV.

the same scale the squared neutron and proton matter form factors, and neutron spin form factor. We see that over the entire energy range the gross features (within a factor of 2) of $d\sigma/d\Omega$ are reflections of the features of the form factors. This is of course expected since single scattering dominates and there is mainly S wave KN scattering. In particular, the first zero in $\rho_{\text{matter}}(q)$ is clearly the cause of the shallow dip in $d\sigma/d\Omega$ at $q^{-2} \simeq 11\ \text{fm}^{-2}$—a

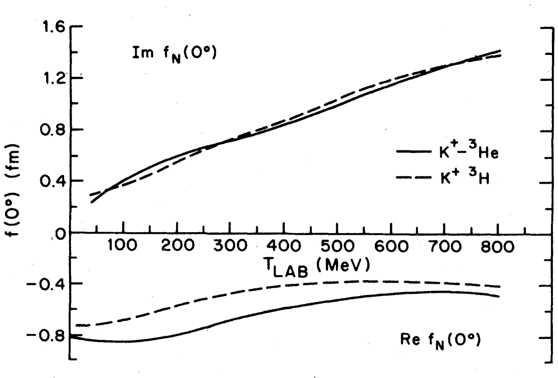

FIG. 7. The real and imaginary parts of the forward, pure strong amplitude for K^+ scattering from ^{3}He and ^{3}H plotted as function of kaon laboratory energy.

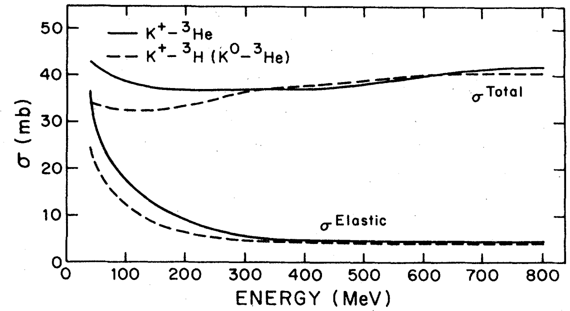

FIG. 8. The total and integrated elastic scattering cross sections for the hadronic scattering of K^+ from ^{3}He and ^{3}H.

dip which, consequently, moves to decreasing angles with increasing energy (see Fig. 9). This zero in $\rho^p_{\text{matter}}(q)$ gets filled by scattering from the neutron matter [Fig. 5(b)], by spin flip scattering from the neutron spin distributions (Fig. 6),

$$(d\sigma/d\Omega)_{\text{unpol}} = |f(\theta)|^2 + \sin^2\theta\,|g(\theta)|^2 \ , \tag{27}$$

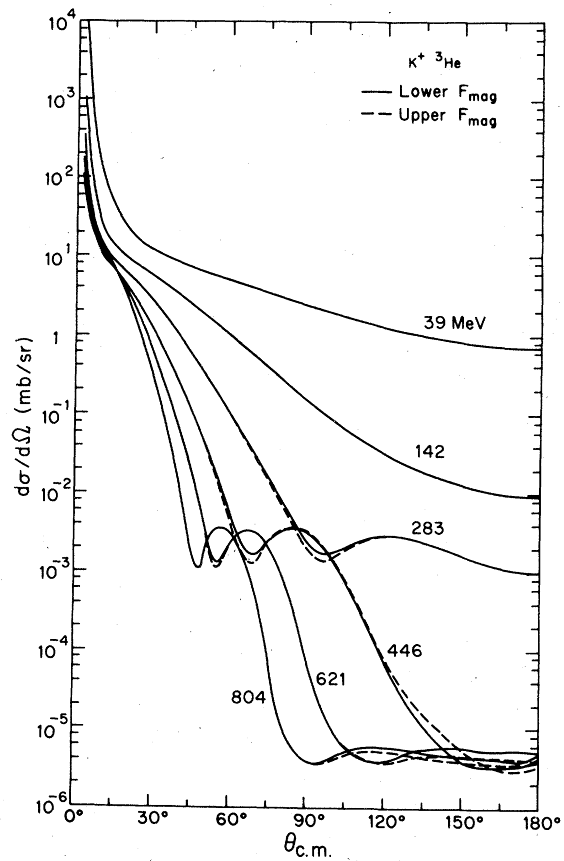

FIG. 9. K^+ ^{3}He elastic scattering for $E = 39-804$ MeV calculated with spin distributions obtained by varying the parameters in the input $F_{\text{mag}}(^3\text{He})$.

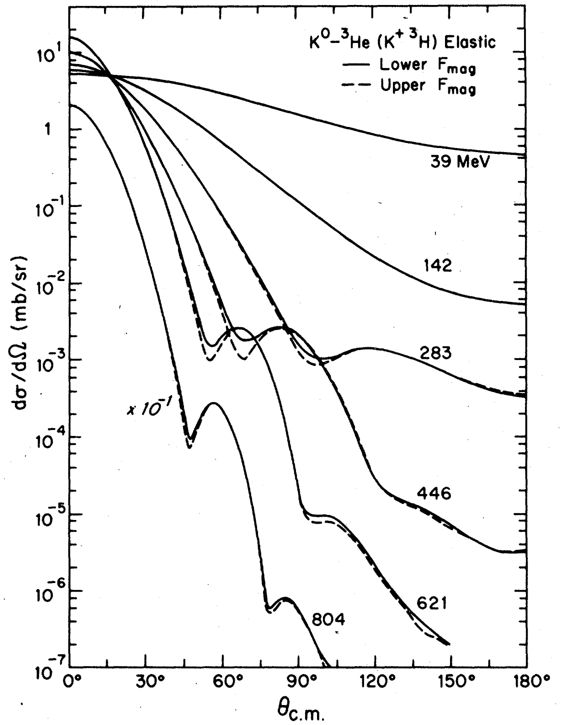

FIG. 10. Same as Fig. 9 except for K^0-^{3}He scattering.

and to a lesser extent (see Fig. 4) by multiple scattering.

Another revealing aspect of Fig. 5(a) is the change in slope and magnitude of the small q^2 cross section as the energy increases. This is a direct consequence of the increasingly important K^+-neutron nonflip, P wave interaction (see Fig. 1). Clearly, at 804 MeV the nonflip t^{Kn} ($l'=1$) get so large that the neutron matter term in the optical potential dominates and consequently the slope of the small q^2 cross section is the same as that of $\rho_{\text{matter}}^2(n)$ [i.e., $F^{\text{charge}}(^3\text{H})^2$]. Thus we have a simple illustration of how a change in the beam energy changes the part of the nucleus producing the scattering.

The general weakness and transparency of the K^+-nucleus interaction is also evident in the K^+*nucleus* phase shifts and absorption parameters. We find that as a consequence of the repulsive K^+p interaction, all the K^+-^{3}He and K^+-^{3}H nuclear phase shifts (we calculate ~ 20) are repulsive, and Ref(0°) (Fig. 7) is uniformly repulsive. In addition there is little absorption ($\eta_L \gtrsim 0.6$). The total and integrated elastic cross sections, shown in Fig. 8 as a function of energy, are also smooth and similar for both nuclei. We note, however, that the theory predicts a rapidly decreasing elastic cross section

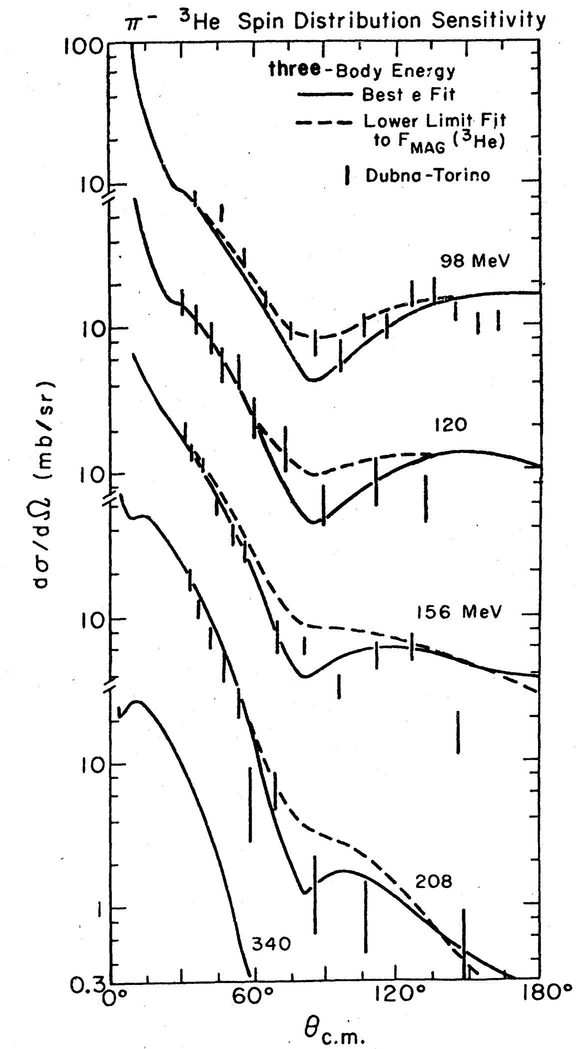

FIG. 11. π^--^{3}He elastic scattering for $E = 98-340$ MeV as calculated with the two spin distributions obtained by using the best fit for $F_{\text{mag}}(^3\text{He})$ and the lower limit fit.

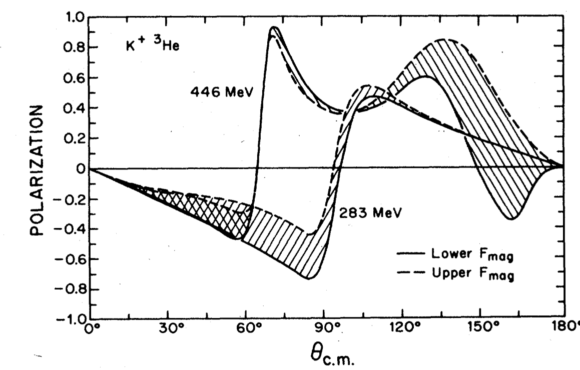

FIG. 12. Polarization of recoiling nucleus in K^+-^{3}He elastic scattering at 283 and 446 MeV. The bands are generated by varying the parameters in the input $F_{\text{mag}}(^3\text{He})$.

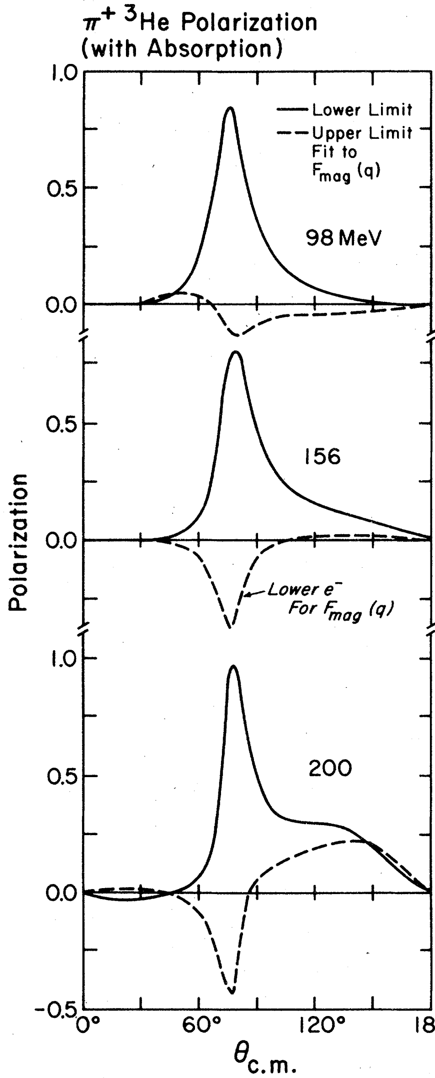

FIG. 13. Same as Fig. 12 except now for π^+ scattering.

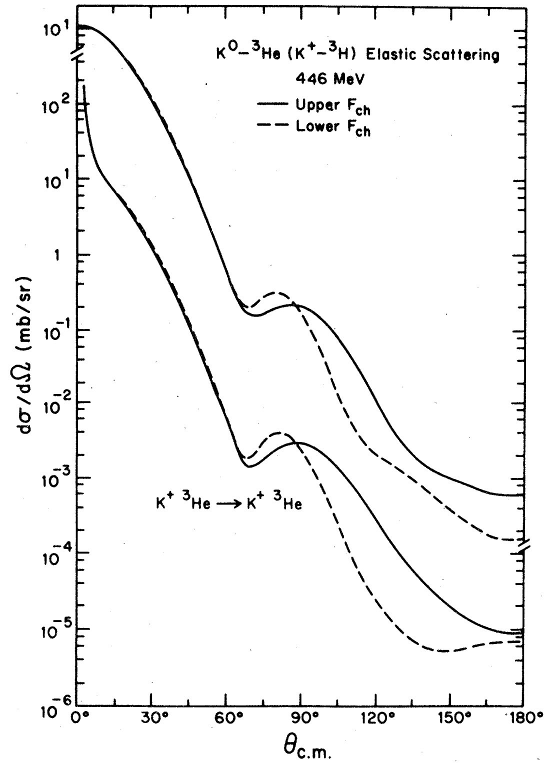

FIG. 14. K^+-^{3}He and K^0-^{3}He elastic scattering at 446 MeV calculated with upper and lower values for the input *charge* form factor $F_{ch}(^3\text{He})$.

and consequently most of the total cross section for $E \gtrsim 100$ MeV arises from quasielastic scattering and π production (our input KN phases can be complex). Elastic scattering is clearly strongest at low energies. Finally, these total cross sections are not sensitive to small changes in the nuclear size; they vary by $\sim 3\%$ for $a \sim 15\%$ change in the neutron radius.

C. Structure sensitivity

In order to study the sensitivity of K^+-^{3}He, ^{3}H scattering to the nuclear structure, we ran our computer code using the ^{3}He form factors of Eq. (24) but not with the best fit parameters. Instead, we employ what we call the "upper" and "lower" limits of the electron scattering fits arrived at by evaluating the form factors with all their parameters at their respective upper and lower limits (e.g., $a_m = 0.654 \pm 0.024 = 0.678, 0.630$). While this is not a statistically significant measure of the error in the electron scattering measurements, it produces a variation in our predictions which indicates the sensitivity of (uncertainty in) the calculation caused by the uncertainty in the input nuclear sizes.

In Fig. 9 we note that K^+ ^{3}He elastic scattering shows its largest sensitivity to the above variation of the neutron spin distribution [i.e., the input $F_{mag}(^3\text{He})$] in the region of the first minimum and for medium energies, $300 \lesssim T_K \lesssim 600$ MeV. Likewise in Fig. 10 we see that K^+-^{3}H (K^0-^{3}He) scattering shows a somewhat higher sensitivity to the neutron spin distribution. We would like to remind the reader that while studying Figs. 4–6, 9, and 10 she should keep in mind that the large angle scattering at these higher energies involve very large momentum transfers ($q \simeq$ fm^{-1}). As such, the input nuclear form factors are being evaluated at momentum transfers which frequently exceed those measured in electron scattering and consequently we have either an excellent probe of these form factors or a large degree of uncertainty in the calculation.

A revealing contrast to the K^+ scattering shown in Figs. 9 and 10 is the π^--^{3}He elastic scattering shown in Fig. 11. We see firstly that the dip in $d\sigma/d\Omega$ (π-^{3}He) does *not* changes its angular position with increasing energy. This is a consequence of the elementary P_{33} eigenchannel truly dominating the scattering (the 90° dip in the πN c.m. gets thrown forward in the π-He c.m.) and the large amount of multiple scattering (so we see more than just the form factor). In K^+ ^{3}He scattering the dip is approximately at a constant value of q^2 and thus moves inwards with energy. Secondly, we can see from Figs. 9 – 11 that π^--^{3}He scattering is ~ 20 times larger, and shows more spin sensitivity than K^+ scattering. In contrast, pion scattering is known to be sensitive to some higher order corrections in the theory,[22] whereas these same corrections have been estimated to be quite low for K^+ scattering[3,4]—a fact corroborated by the small multiple scattering contribution.

Probably the most direct way to observe spin effects in scattering from the three nucleon system is to use a polarized target or to measure the recoil polarization of the nucleus. In Fig. 12 we display our predictions for this polarization at 283 and 446 MeV for two sizes of the spin distribution. We see that beyond $\sim 45°$ the polarizations get quite large and quite energy dependent. The sensitivity to the spin distribution is higher than that found for π^- ^{3}He (π^+ ^{3}H) scattering but as seen in Fig. 13, not as high as found for π^+ ^{3}He (π^- ^{3}H) scattering.

In Fig. 14 we examine the sensitivity of K^+-^{3}H and K^+-^{3}He scattering at 446 MeV to variations in the input *charge* form factor of ^{3}He, Eq. (24). As Eqs. (20) – (23) indicate, this will affect both matter and spin form factors, and as Figs. 14, 17, and 18 indicate, it has a large effect on K^+ scattering especially for $\theta \gtrsim 90°$. It is interesting to note that this senistivity to the proton distribution arises from a conjunction rather unique to K^+'s: On the one hand, the beam momentum is high enough (800 MeV/c) to obtain momentum transfers large enough ($q \lesssim 8$ fm^{-1}) to explore the form factors in a region of uncertainty; on the other hand, the KN interaction is of such short range that even at this high beam momentum it is still the S-wave K^+-proton amplitude which dominates (see Figs. 1 and 2). In contrast, for the pion probe, both isospin channels (and many more partial waves) would contribute more or less equally at this high a beam momentum.

D. Isotopic effects

If kaon-nucleus scattering is to be used to deduce reliable nuclear structure information then it is important to employ procedures which minimize the uncertainties in the theory and in the experiments. One technique, employed by Nefkins *et al.*,[32] is to examine the ratio $(d\sigma/d\Omega)$ (π^+ ^{3}He)/$(d\sigma/d\Omega)$ (π^- $^3\text{He} \equiv \pi^+$ ^{3}H) as a function of angle. In this case, the theoretical ratio agrees better with the experimental ratio than the individual cross sections. Likewise, Johnson *et al.*[33] have found that the experimental ratio $(d\sigma/d\Omega)$ (π^- ^{18}O)/$(d\sigma/d\Omega)$ (π^- ^{16}O) can be used to deduce the difference in rms radii of the neutron distribution in the isotope pair—with results which are essentially model independent. And finally, it has been known for quite some time[34] that the relative differences in electron scattering cross sections can be determined very accurately and then used to deduce accurate differences in charge densities.

Motivated by the above techniques, we present our results in a form which shows the nuclear size sensitivity in terms of isotopic ratios and differences. In Fig. 15 we plot the ratio of cross sections for 446 MeV K^+ scattering from ^{3}He and ^{3}H for different input magnetic form factors, and in Fig. 16 we plot the relative isotopic difference

$$D(\theta) = \left[\frac{d\sigma}{d\Omega}(^4\text{He}) - \frac{d\sigma}{d\Omega}(^3\text{He})\right] \Big/ \left[\frac{d\sigma}{d\Omega}(^4\text{He}) + \frac{d\sigma}{d\Omega}(^3\text{He})\right] . \tag{28}$$

We see that K^+-^{3}He scattering is generally larger than K^+ ^{3}H scattering—this being a consequence of the large K^+p S-wave interaction at this energy (Fig. 1). Near 60° and 150°, however, the cross section has minima and the spin flip scattering makes K^+ ^{3}H larger and introduces some sensitivity to the neutron spin distribution. If K^+ scattering from ^{3}He and ^{4}He are compared, Fig. 16, we find sensitivity only for $\theta \gtrsim 130°$. Yet as we see in Figs. 17 and 18, $R(\theta)$ and $D(\theta)$ for $\theta \gtrsim 90°$ are much

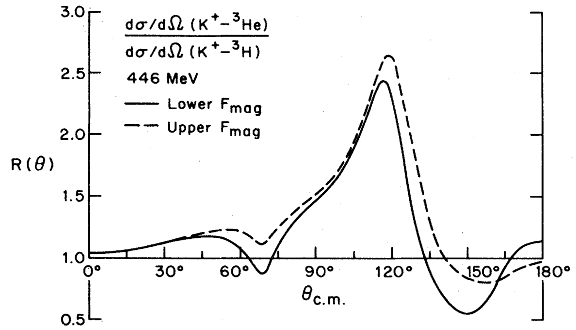

FIG. 15. The ratio of the differential cross sections for K^+ elastic scattering from ^{3}He and ^{3}H at 446 MeV. The two curves result from assuming the upper and lower limits to the size of the input magnetic form factor of ^{3}He.

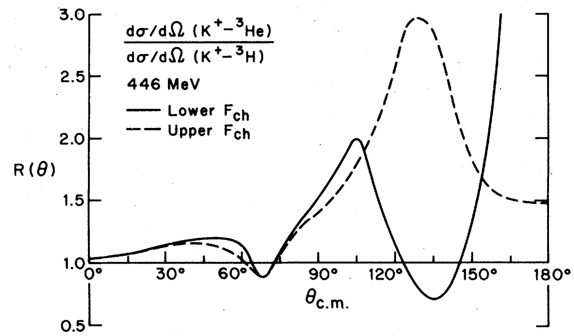

FIG. 17. The same as Fig. 15 except now for the charge form factors.

more sensitive to the uncertainty in the ^{3}He *charge* form factor than in the magnetic one.

IV. SUMMARY AND CONCLUSIONS

We have extended our momentum space optical potential formulation to permit the study of the elastic and charge exchange scattering of K^+ and K^0 mesons from spin 0 and spin $\frac{1}{2}$ nuclei for beam energies $0 < T_K \lesssim 1$ GeV. Our formulation thus includes the KN *S-F* wave spin-dependent scattering amplitudes, a separable potential model to generate their off-shell behavior, an accurate description of off-shell kinematics and transformations, and realistic form factors to describe the nuclear distribution of matter and spin. In the work reported here we present differential cross sections, total cross sections,and polarizations for K^+ elastic scattering from ^{12}C, ^{4}He, ^{3}He, and ^{3}H, and make several comparisons to related results obtained in pion scattering.

We find that our parameter-free calculations reproduce the angular dependence of the 446 MeV K^+-^{12}C cross section recently measured by a CMU-Houston-BNL group,[10,31] but underestimates the small angle data by approximately a factor of 2. Although our calculations do exhibit sensitivity to a number of theoretical assumptions and to the empirical input, it does not appear large enough to remove this discrepancy. Since higher order corrections are expected to be small, we consider this an important open question.

Since the three nucleon system contains a good

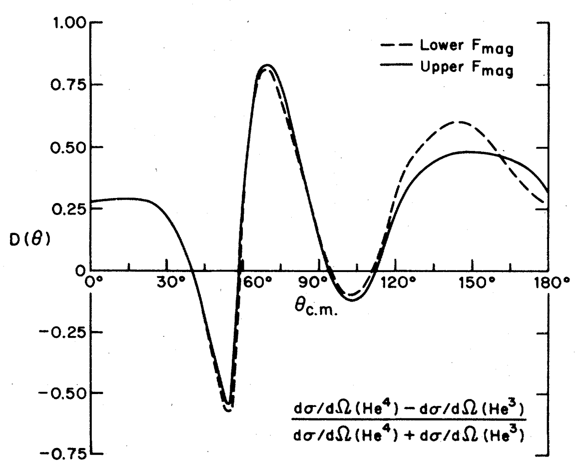

FIG. 16. The relative difference in K^+ scattering from ^{3}He and ^{4}He at 446 for the upper and lower values for $F_{mag}(^3He)$.

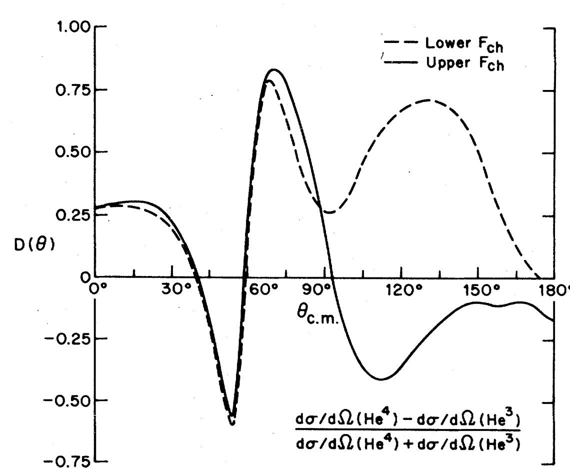

FIG. 18. The same as Fig. 16 except now for the charge form factors.

deal of interesting nuclear structure, with much of it at the hard-to-determine few percent level, we have explored how the kaon might complement the electron and pion as probes of this structure. We found that K^+-^{3}H scattering displays more sensitivity than K^+-^{3}He scattering to the distribution of neutron spin in the nucleus, although it is still significantly less than shown for pions. However, since K^+ scattering is ~ 20 times weaker than pion scattering, we expect that many of the "higher order corrections" which introduce uncertainties into pion scattering will not be present for K^+'s. Quite possibly, the relatively high sensitivity of K^+-^{3}He and K^+-^{3}H scattering to uncertainties in the n and p *matter* distributions [$F_{ch}(^3\text{H})$ and $F_{ch}(^3\text{He})$] will permit the K^+ to complement the electron in probing the high momentum transfer components of the matter (charge) form factors, with fewer questions concerning the contributions from meson exchange currents. In this regard, as shown in our last figure, a measurement of the ratio of large angle cross sections for different isotopes seems promising for beam energies in the range 300 − 500 MeV.

ACKNOWLEDGMENTS

We would like to thank Dr. E. Hungerford for suggesting this study, for a number of helpful conversations, and for supplying the preliminary K^+-^{12}C data. Helpful conversations with Dr. F. Tabakin, Dr. S. Cotanch, Dr. G. Walker, and Dr. C. Dover are also acknowledged and appreciated. This work was supported in part by the National Science Foundation, The Oregon State University Computer Center, La Universidad de Antioquia, and the OSU Research Council.

---

*On leave from Departmento de Física, Universidad de Antioquia, Medellín, Colombia.

[1]R. J. Abrams, R. L. Cool, G. Giacomelli, T. F. Kycia, K. K. Liand, and D. N. Michael, Phys. Lett. 30B, 564 (1969); D. V. Bugg, R. S. Gilmore, K. M. Knight, D. C. Slater, G. H. Stafford, E. J. N. Wilson, J. D. Davies, J. D. Dowell, P. M. Hattersley, R. J. Homer, A. W. O'Dell, A. A. Carter, R. J. Tapper, and K. F. Riley, Phys. Rev. 168, 1466 (1968).

[2]G. Fäldt and T. E. O. Ericson, Nucl. Phys. B8, 1 (1968); J. Pumplin, Phys. Rev. 173, 1651 (1968); R. H. Landau, Phys. Rev. D 3, 81 (1971).

[3]C. B. Dover and P. J. Moffa, Phys. Rev. C 16, 1087 (1977).

[4]C. B. Dover and G. E. Walker, Phys. Rev. C 19, 1393 (1979).

[5]*Meson-Nuclear Physics—1979 (Houston),* Proceedings of the 2nd International Topical Conference on Meson-Nuclear Physics, edited by E. V. Hungerford III (AIP, New York, 1979).

[6]S. R. Cotanch and F. Tabakin, Phys. Rev. C 15, 1379, (1977).

[7]S. R. Cotanch, Phys. Rev. C 18, 1941 (1978); Nucl. Phys. A308, 253 (1978); Phys. Rev. C 21, 2115 (1980).

[8]S. R. Cotanch, Phys. Rev. C 23, 807 (1981),

[9]A. S. Rosenthal and F. Tabakin, Phys. Rev. C 22, 711 (1980).

[10]*Proceedings of the Kaon Factory Workshop, Vancouver 1979,* edited by M. K. Craddock (TRIUMF, Vancouver, 1979).

[11]A. W. Thomas, Invited Talk, International Conference on Nuclear Physics, Berkeley, 1980 (unpublished).

[12]R. H. Landau, S. C. Phatak, and F. Tabakin, Ann. Phys. (N.Y.) 78, 299 (1973).

[13]R. H. Landau, Ann. Phys. (N.Y.) 92, 205 (1975); Phys. Rev. C 15, 2127 (1977).

[14]R. H. Landau, LAMPF Report LA-7892-C, 150 (1979).

[15]Y. Alexander and R. H. Landau, Phys. Lett. 84B, 292 (1979).

[16]Since there has been some question concerning the use of momentum space codes for the very large momentum transfers obtained with kaons (Ref. 10) we have checked our numerical procedures by calculating the form factor $F(q)$ analytically and comparing these results with those obtained by summing the Legendre polynomial series for $F(q)$. The sum appeared accurate to at least three places out to $q^2 \simeq 30\ \text{fm}^{-2}$.

[17]M. Paez and R. H. Landau, Phys. Rev. C (to be published).

[18]B. R. Martin, Nucl. Phys. B94, 413 (1975); S. J. Watts, D. V. Bugg, A. A. Carter, M. Coupland, E. Eisenhandler, A. Astburg, G. H. Grayer, A. W. Robertson, T. P. Shah, and C. Sutton, Queen Mary and Rutherford report.

[19]J. H. Hetherington and L. H. Schick, Phys. Rev. 138, B1411 (1965).

[20]G. Giacomelli *et al.* Nucl. Phys. B71, 138 (1974) (BGRT).

[21]C. Dover, private communication.

[22]A. W. Thomas and R. H. Landau, Phys. Rep. 58, 121 (1980); Nucl. Phys. A302, 461 (1978).

[23]R. Aaron, R. D. Amado, and J. E. Young, Phys. Rev. 174, 2022 (1968).

[24]R. F. Frosch, J. S. McCarthy, R. E. Rand, and M. R. Yearin, Phys. Rev. 100, 879 (1967).

[25]B. Bartoli, F. Felicetti, and V. S. Silvestrini, Rev. Nuovo Cimento 2, 241 (1972).

[26]I. Sick and J. S. McCarthy, Nucl. Phys. A150, 631

(1970).

[27] L. I. Schiff, Phys. Rev. 133, B802 (1964); B. F. Gibson and L. I. Schiff, Phys. Rev. 138, B26 (1965).

[28] J. S. McCarthy, I. Sick, R. R. Whitney, and M. R. Yearian, Phys. Rev. Lett. 25, 884 (1970).

[29] H. Collard, R. Hofstadter, E. B. Hughes, A. J. Johansson, M. R. Yearian, R. B. Day, and R. T. Magner; Phys. Rev. 138, B57 (1965).

[30] M. McMillan, Phys. Rev. C 3, 1702 (1971).

[31] E. V. Hungerford, in the *9th International Conference on Few Body Problems, Eugene,* edited by F. S. Levin (North-Holland, Amsterdam, 1981) [special edition, Nucl. Phys. A353, 75C (1981)]; and private communication.

[32] B. M. K. Nefkens, in *Few Body Systems and Nuclear Forces,* edited by H. Zingl *et al.* (Springer, Berlin, 1978), Vol. II; P. Glodis *et al.*, Phys. Rev. Lett. 44, 234 (1980).

[33] R. R. Johnson, T. Masterson, B. Bassalleck, W. Gyles, T. Marks, K. L. Erdman, A. W. Thomas, D. R. Gill, E. Rost, J. J. Kraushaar, J. Alster, C. Sabev, J. Arvieux, and M. Krell, Phys. Rev. Lett. 43, 844 (1979).

[34] R. F. Frosch, R. Hofstadter, J. S. McCarthy, G. K. Nöldeke, K. J. Van Oostrom, B. C. Clark, R. Herman, and D. G. Ravenhall, Phys. Rev. 174, 1380 (1968).